

# Transport and Mechanical Properties of iPP–sPP Fibers

G. GORRASI,<sup>1</sup> V. VITTORIA,<sup>1</sup> P. LONGO<sup>2</sup>

<sup>1</sup> Dipartimento di Ingegneria Chimica e Alimentare—Università di Salerno, Via Ponte don Melillo, 84084 Fisciano (Salerno), Italy

<sup>2</sup> Dipartimento di Chimica—Università di Salerno, Via Salvator Allende, 84080 Baronissi (Salerno), Italy

Received 6 March 2000; accepted 12 June 2000

**ABSTRACT:** The drawing behavior of a blend of syndiotactic and isotactic polypropylene (iPP–sPP 50:50 w/w) was investigated at different temperatures and compared to that of pure polymers. The film of pure sPP showed that the presence of iPP allowed the blend to reach a much higher draw ratio. Fibers were obtained by drawing the blend at 110°C. The axial elastic modulus of the fibers was measured as a function of draw ratio up to the highest  $\lambda = 10$ . The sorption and diffusion of dichloromethane vapors in the undrawn and drawn samples were studied in order to provide information about the structural organization of the amorphous phase. The elastic modulus of the fibers displayed a more-than-linear increase with the draw ratio, suggesting a good interconnection of the amorphous phases. The orientation of the chains with increasing  $\lambda$  determined a decrease of entropy and fractional free volume (FFV) and a tighter packing of the chains along the drawing direction, explaining the strong increase of the elastic modulus. The transport properties, which confirmed the mechanical properties, showed a stiffening of the amorphous phase after  $\lambda = 6$ , evidenced by a dual-type sorption isotherm for the fibers and a sharp drop in the zero-concentration diffusion coefficient. As a consequence, the permeability of the fibers was much lower than that of the unoriented sample. © 2001 John Wiley & Sons, Inc. *J Appl Polym Sci* 80: 539–545, 2001

**Key words:** iPP; sPP; blend; fibers; transport properties

## INTRODUCTION

The possibility of obtaining polyolefin with different configurations (atactic, isotactic, and syndiotactic) is very interesting, both from the theoretical and from the technological point of view. As matter of the fact, different tacticities in stereoregular polymers produce different structural organizations and, as a consequence, very different physical and mechanical properties. Furthermore, it is possible to clarify the relationships between structure and properties because of the

differing spatial configuration of the substituents along the molecular chain.

Recently metallocene catalysts were successfully used in order to produce polypropylene with new tacticity microstructures, in particular, syndiotactic chains with a wide range of tacticities and molecular weights.<sup>1–3</sup> These chain structures significantly increase the possibility of exploring new properties beyond those of conventional isotactic polypropylene, and, therefore, many investigations of them have been reported.<sup>4–13</sup> Although syndiotactic polypropylene displays interesting properties, some of its aspects show a poorer behavior than an isotactic isomer, including a slow crystallization rate and a very complicated polymorphism, not yet fully clarified. Fur-

Correspondence to: V. Vittoria (vittoria@post.dica.unisa.it).

*Journal of Applied Polymer Science*, Vol. 80, 539–545 (2001)  
© 2001 John Wiley & Sons, Inc.

thermore, in relation to isotactic isomer, sPP has worse tensile properties: in fact, depending on the starting structure and on the drawing temperature, the maximum achievable draw ratio is about 5–7, significantly lower than that of iPP.<sup>14–18</sup> The poor ductility of sPP has been ascribed to the absence of a crystalline relaxation, which has instead been clearly observed in the highly drawable iPP.<sup>14</sup> Drawing increases the orientation of the chains, greatly improving the mechanical properties of polymers, and it is therefore highly desirable. In some cases, blending can improve particular characteristics of a polymer component. It has been shown that blending sPP with iPP or aPP improves some properties, and blending with HDPE greatly increases the crystallization kinetics.<sup>19–23</sup>

In this article we show the results obtained by blending syndiotactic and isotactic polypropylene at a composition of 50:50 w/w. We investigated this possibility in order to better orient the syndiotactic isomer, thus achieving high draw ratios. It has been already shown that iPP and sPP are incompatible even in the melt state.<sup>19</sup> They undergo liquid–liquid phase separation in the melt, producing either isotactic PP in a syndiotactic matrix or sPP in an isotactic matrix, depending on the composition, while a cocontinuous morphology was reported for nearly symmetric blends.<sup>19</sup> We obtained high draw ratios and studied the mechanical and transport properties of the obtained fibers. In blends and in oriented polymers, a major problem is the state of the amorphous phase or phases, and few methods are available for this purpose. Transport properties are particularly suited to an investigation of the amorphous phase: as a matter of fact, they are related to the fraction and to the thermodynamic state of this phase and can give valuable information about its role in the deformation process and in final properties. Previous investigations of the uniaxial deformation of linear high-density polyethylene,<sup>24</sup> low-density polyethylene,<sup>25–26</sup> linear low-density polyethylene,<sup>27</sup> and isotactic polypropylene,<sup>28–30</sup> have revealed the usefulness of transport properties for this purpose.

## EXPERIMENTAL

### Materials

The isotactic polypropylene (iPP) used in this work was a product of Rapra (United Kingdom)

with  $M_n = 15,600$  and  $M_w = 307,000$ . The syndiotactic polypropylene (sPP) was synthesized according to a previous procedure<sup>12</sup>; it showed 91% of syndiotactic pentads, as evaluated by nuclear magnetic resonance (NMR). A blend of the two polymers was obtained by codissolving the two materials (50:50 w/w) using toluene at high temperature and then precipitating the powders with cold methanol. After 3 days under vacuum, the powders were molded in a hot press at 190°C, and cooled in an ice-water bath (0°C) for 1 min, producing a film 0.1 mm thick. The film was submitted to drawing processes at several temperatures (25°C, 50°C, 80°C, 110°C, and 130°C) in order to choose the best temperature for achieving high draw ratios. Since either isotactic and syndiotactic polypropylene quenched from the melt undergoes a strong aging phenomenon,<sup>12,31</sup> we normalized the elapsed time from the quenching by drawing the blend after 24 h.

### Methods of Investigation

The stress–strain curves of the starting film at different temperatures, the preparation of the fibers at different draw ratios, and the evaluation of the elastic modulus were performed using an Instron 4301 dynamometer, equipped with a thermostatic camera for high temperatures.

The drawing rate was 10 mm/min on samples that had an initial length of 10 mm.

The elastic modulus of the fibers and of the undrawn blend was detected at 25°C within the linear trend (deformation less than 1%) of the stress–strain curve. The detected values were averaged over 10 measurements.

The fibers prepared at 110°C at different  $\lambda$  were cooled to room temperature before being unhooked from the testing device. The samples were placed in a dichloromethane atmosphere at varying-activity  $a = P/P_0$  of vapor, where  $P$  is the actual vapor pressure and  $P_0$  is the saturation pressure of vapor at the temperature of the experiment:  $T = 25^\circ\text{C}$ .

The transport properties (sorption and diffusion) were then measured according to a previously described microgravimetric method,<sup>25</sup> using a quartz spring balance having an extension of 16 mm/mg.

Wide-angle X-ray diffractograms (WAXD) were obtained using a Philips PW 1710 Powder diffractometer ( $\text{CuK}\alpha$ -Ni filtered radiation). The scan rate was  $2^\circ/\text{min}$ .

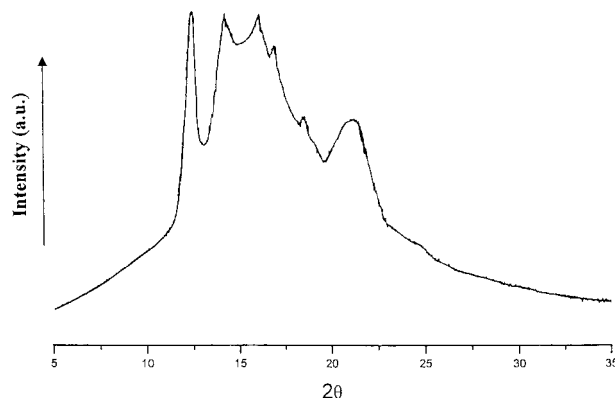


**Figure 1** The X-ray diffractogram of the 50:50 iPP-sPP blend, film quenched at 0°C.

## RESULTS AND DISCUSSION

### Mechanical Properties

Figure 1 shows the wide-angle X-ray diffractogram of the 50:50 iPP-sPP blend. As already reported,<sup>19</sup> and which was also true in our case, the two polymers crystallized separately in their usual crystalline forms. As matter of fact, the diffractogram is composed solely of iPP and sPP crystalline contributions: the  $\alpha$  monoclinic form of iPP, characterized by main peaks at 14.1°, 16.8°, 18.4°, and 21° of  $2\theta$  for isotactic PP, and the most usual form of syndiotactic PP, referred to in the literature as form I,<sup>7</sup> showing the most intense peaks at 12.4° and 15.9° of  $2\theta$ . The lack of a peak at 18.8° of  $2\theta$  for syndiotactic polypropylene reveals that we obtained the disordered form I. The crystalline peaks, although clearly distinguishable, have shifted substantially on the baseline, indicating a poor crystallinity of both polymers and a large amorphous fraction. It has been shown that in blends of iPP and sPP, crystallization temperature is a stronger determinant of the rate of crystallization for iPP than for sPP. Thus, with higher degrees of supercooling, crystallization of iPP is faster, while with lower supercooling sPP crystallizes faster.<sup>19</sup> It is worth recalling that we quenched the blend at 0°C and that under these conditions isotactic PP generally solidifies in the smectic form.<sup>32</sup> In the presence of sPP a variant was obtained—the monoclinic form of iPP, although of low crystallinity.

The 50:50 blend of iPP-sPP was submitted to various stress-strain treatments at different temperatures in order to detect the best temperature to be used for obtaining the highest draw ratios.

Figure 2 displays the stress-strain curves obtained at 25°C (curve A), 50°C (curve B), 80°C (curve C), 110°C (curve D), and 130°C (curve E). At 25°C the drawing behavior was found to be typical of a semicrystalline system, which deforms through neck propagation. According to Hooke's law, at the beginning the stress is proportional to the deformation; after the yield point and for the drop after the yield, we had a range of almost constant stress, in which the starting morphology of the samples was transformed into a fibrillar morphology. When most of the oriented fibrils were aligned, a bigger stress for small deformations was needed, and we observed a climbing of the curve to the break (strain hardening). However, at 25°C and 50°C a sharp yield point was evident, showing that increasing the drawing temperature leads to a progressive reduction of the sharp yield point, until it completely disappears at 110°C and 130°C. The deformation becomes more and more homogeneous, and the drawing ratio results increased. This behavior was verified up to  $T = 110^\circ\text{C}$ , the temperature at which we observed the highest draw ratio. From this temperature up to 130°C, the trend results are inverted, and the sample breaks earlier. This temperature is, in fact, sufficiently high enough to determine the partial melting of sPP, with loss of continuity in the morphological elements submitted to drawing. The sample breaks very early.

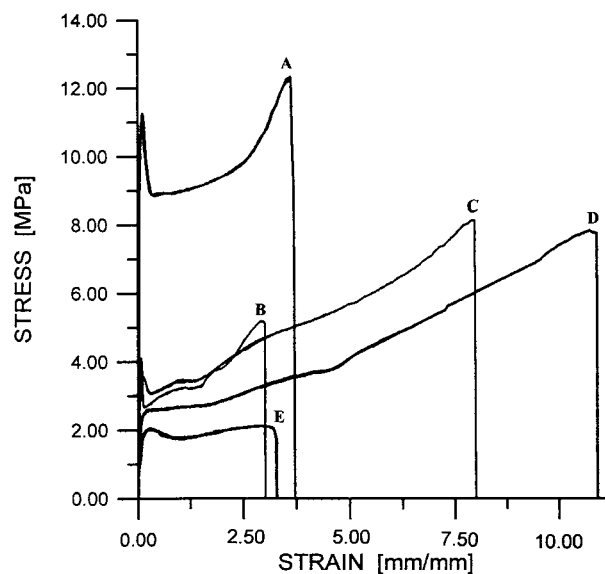


**Figure 2** Stress-strain curves obtained at different temperatures for the 50:50 iPP-sPP blend—curve A: 25°C; curve B: 50°C; curve C: 80°C; curve D: 110°C; curve E: 130°C.

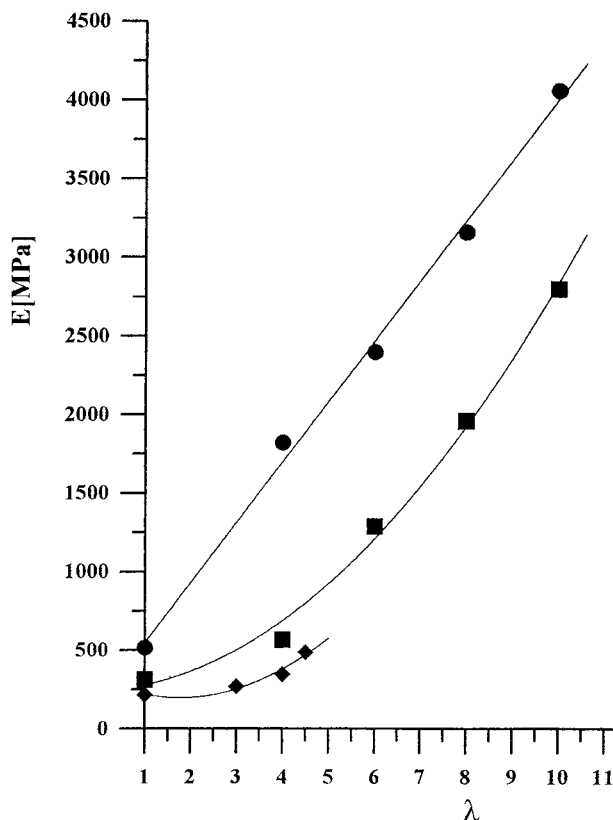


**Figure 3** The elastic modulus [ $E$  (MPa)] as a function of the draw ratio ( $\lambda$ ) for (●) pure iPP, (■) 50:50 iPP-sPP blend, and (◆) pure sPP.

After this preliminary analysis, we decided to prepare the fibers of 50:50 sPP-iPP at  $T = 110^\circ\text{C}$ , considering it the best temperature for drawing the blend. It is worth remembering that  $110^\circ\text{C}$  is the best drawing temperature of isotactic PP.<sup>29,30</sup> At this temperature a lower yield point is not observed, and neck propagation occurs up to  $\lambda = 4$ . After this value of the deformation ratio, when the neck is propagated to the whole sample, strain hardening in the stress-strain curve is observed. The persistence of the neck up to  $\lambda = 4$  prevents intermediate draw ratios from being obtained in the range 1–4. Although syndiotactic polypropylene drawn at room temperature and taken out of the clamps shows a very consistent contraction of the length and a rubberlike behavior,<sup>33</sup> in our case the drawing of the blend at  $110^\circ\text{C}$  did not produce these effects. Contraction of the length was very small, and the fibers did not show elastic behavior.

Figure 3 reports the elastic modulus,  $E$  (MPa) as function of  $\lambda$  for the fibers obtained from the 50:50 sPP-iPP blend compared to those obtained

from the pure polymers. All the fibers obtained at  $110^\circ\text{C}$ , both from the homopolymers and the blend, show a strong aging at room temperature. For comparison, we measured all properties 24 h after the drawing.

It is worth noting that at  $110^\circ\text{C}$  pure sPP reaches a maximum draw ratio equal to 4.5, while when it is blended with iPP, the system can be drawn up to  $\lambda = 10$ . Therefore, the presence of iPP improves the drawability of sPP. For the blend, we observe after  $\lambda = 4$  a more-than-linear increase of modulus, due to the increasing orientation of the amorphous phases, and the progressive formation of tie molecules connecting different crystalline blocks. The drawability of the blend and the quite high modulus obtained for the drawn samples, although lower than pure iPP, are a strong indication of a partial interconnection of the amorphous phases of iPP and sPP. In fact, the good mechanical behavior of the fibers indicates a continuity between the crystalline phase and the connecting amorphous matrix.

### Transport Properties

In order to better investigate the structural organization of the amorphous phases of the fibers, sorption and diffusion parameters were evaluated at different vapor activities, using dichloromethane as a model molecule of penetrant. At each vapor activity the sorption was reported as  $Ct/Ceq$ , where  $Ct$  is the concentration of vapor at time  $t$ , and  $Ceq$  the equilibrium value, as a function of square root of time  $t^{1/2}$ . All the curves were linear in the initial part, following a Fickian behavior, and it was possible to derive a diffusion coefficient,  $D$  ( $\text{cm}^2/\text{s}$ ), from the relation<sup>34–36</sup>:

$$Ct/Ceq = 4/d(Dt/\pi)^{1/2} \quad (1)$$

where  $d$  (cm) is the thickness of the sample.

Since the diffusion coefficient increases with increasing concentration, we have to determine the dependence of diffusion on concentration in order to extrapolate to the zero penetrant concentration and obtain the thermodynamic parameter  $D_0$ , which is related to the fractional free volume (FFV) and to the tortuosity of the path, due to the impermeable phase or phases. Generally, the dependence of diffusion on penetrant concentration is of the exponential form:

$$D = D_0 \exp(\gamma Ceq) \quad (2)$$

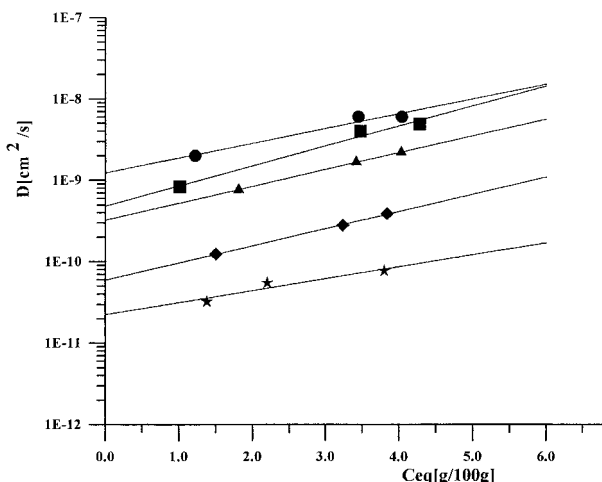


**Figure 4** The diffusion coefficient [ $D$  ( $\text{cm}^2/\text{s}$ )] as a function of  $C_{eq}$  ( $\text{g}/100 \text{ g}$ ) of dichloromethane sorbed by the undeformed film of the (●) 50:50 iPP-sPP blend  $\lambda = 1$  and the samples drawn to (■)  $\lambda = 4$ , (▲)  $\lambda = 6$ , (◆)  $\lambda = 8$ , and (★)  $\lambda = 10$ .

where  $\gamma$  is the concentration coefficient, also related to the fractional free volume and to the effectiveness with which the penetrant plasticizes the polymeric system.

In Figure 4 the  $D$  ( $\text{cm}^2/\text{s}$ ) values, as a function of the  $C_{eq}$  ( $\text{g}/100 \text{ g}$ ) of vapor sorbed, are reported for the initial undrawn blend ( $\lambda 1$ ) and for the fibers with different draw ratios ( $\lambda 4$ ,  $\lambda 6$ ,  $\lambda 8$ ,  $\lambda 10$ ). The diffusion results are dependent on concentration, according to eq. (2) and for each draw ratio it was possible to determine the zero diffusion coefficient and the  $\gamma$  coefficient, as reported in Table I. First of all, an interesting result can be observed in that the diffusion of the blend follows very nearly the diffusion of the pure polymers, producing an extrapolated  $D_0$  value of  $1.23 \times 10^{-9}$ , very similar to those of sPP ( $1.80 \times 10^{-9}$ ) and pf iPP

**Table I** Zero Concentration Diffusion Coefficients of Pure Polymers and Blend and Drawn Samples

Sample	$D_0$ ( $\text{cm}^2/\text{s}$ )
iPP	$2.20 \times 10^{-9}$
sPP	$1.80 \times 10^{-9}$
iPP-sPP 50 : 50 $\lambda 1$	$1.23 \times 10^{-9}$
iPP-sPP 50 : 50 $\lambda 4$	$4.85 \times 10^{-10}$
iPP-sPP 50 : 50 $\lambda 6$	$3.27 \times 10^{-10}$
iPP-sPP 50 : 50 $\lambda 8$	$5.95 \times 10^{-11}$
iPP-sPP 50 : 50 $\lambda 10$	$2.26 \times 10^{-11}$

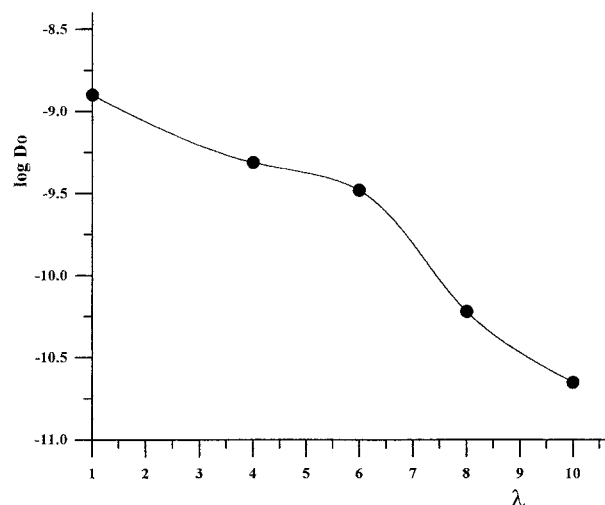


**Figure 5** The logarithm of the zero diffusion coefficient  $D_0$  as a function of the draw ratio  $\lambda$ .

( $2.20 \times 10^{-9}$ ). This is again an indication of good interpenetration and continuity of the amorphous phases, yielding a matrix with the same diffusional properties as the parent polymers. Furthermore, a decrease of diffusion of 2 orders of magnitude is observable on increasing the draw ratio, as already reported for iPP.<sup>30</sup>

Figure 5 displays the log of  $D_0$  as a function of  $\lambda$ . Clearly evident is a smooth decrease of diffusion up to  $\lambda = 6$ , and then a sharp drop between  $\lambda = 6$  and  $\lambda = 8$ . The decrease of  $D_0$  with  $\lambda$ , already found in polyethylene, both high density<sup>24</sup> and low density,<sup>25-27</sup> and in polypropylene,<sup>28,30</sup> can be explained very well in terms of structural changes caused by the drawing process. According to Peterlin's model, the original unoriented lamellar structure is gradually transformed into a highly oriented microfibrillar structure. The microfibrils consist of folded-chain crystalline blocks axially connected by a great many tie molecules passing and compressing the amorphous layers separating the crystal cores of subsequent blocks. The increase of the specific density of the amorphous layers causes a large decrease in their fractional free volume (FFV), which influences the transport properties, in particular the diffusion coefficient. The sharp decrease of the diffusion parameter increasing the draw ratio indicates that the orientation of the amorphous chains and the number of extended tie molecules greatly increase in the interval of the draw ratio between  $\lambda = 6$  and  $\lambda = 8$ . This result, very similar to that obtained for isotactic polypropylene,<sup>30</sup> again indicates a good interpenetration of the amorphous phases.

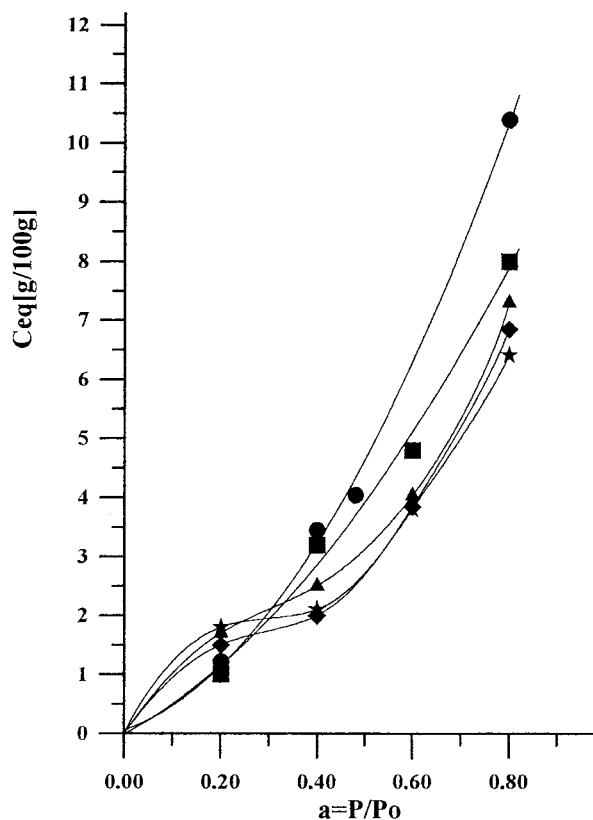


**Figure 6** The equilibrium concentration of dichloromethane  $C_{eq}$  (g/100 g) as a function of vapor activity  $a = P/P_0$  for the undeformed film of the 50:50 iPP-sPP (●) blend  $\lambda = 1$  and the samples drawn to (■)  $\lambda = 4$ , (▲)  $\lambda = 6$ , (◆)  $\lambda = 8$ , and (★)  $\lambda = 10$ .

Figure 6 reports the equilibrium concentration [ $C_{eq}$  (g/100 g)] as a function of vapor activity ( $a = P/P_0$ ) for all the drawn samples and for the undeformed one. It is clearly evident that the sorption modes are quite different. The undrawn sample ( $\lambda 1$ ) and the one drawn up to  $\lambda = 4$ , after a linear behavior, show a positive deviation from Henry's law. This mode of sorption represents a preference for penetrant-penetrant pairs to be formed, so that the solubility coefficient increases continuously with pressure. This behavior depends on the ability of the solvent to plasticize the polymeric matrix and can be interpreted by the Flory-Huggins theory. When the draw ratio increases, the sorption mode is significantly modified. As shown in Figure 6, the sorption curves of samples drawn at draw ratios equal to 6, 8 and 10 ( $\lambda 6$ ,  $\lambda 8$ , and  $\lambda 10$ ) display a region of negative curvature and, after a given value of vapor pressure, a positive deviation from linearity. Such a "dual-type" sorption behavior is typical of glassy

polymers and indicates that higher vapor concentrations are needed to plasticize the polymeric matrix. The sorption is visualized as a process in which there are dual modes: either the penetrant molecules are normally dissolved and free to diffuse, or they are immobilized in particular sites of the polymeric matrix. Such a behavior, appearing for higher draw ratios, can be imputed to a reduction of free volume (FFV), which occurred during the drawing, accompanied by a decrease of segmental mobility and a broader  $T_g$  distribution in the amorphous phase that influences the sorption mode and, as already shown, the diffusional behavior.

## CONCLUSIONS

Isotactic and syndiotactic polypropylene were blended and quenched from the melt state. X-ray analysis showed that the two polymers in the blend crystallize in their usual crystalline forms, although in very disordered and small crystals. The presence of the isotactic isomer greatly increases the drawability of the syndiotactic one, and it was possible to draw the original film up to  $\lambda = 10$  at  $110^\circ\text{C}$ .

The drawing transforms the original lamellar structure into the final microfibrillar one, and the transformation is particularly fast after  $\lambda = 6$ , as determined by transport properties. The axial elastic modulus increases faster with the draw ratio in the blend fibers than in the samples drawn from the pure iPP. The denser packing of the amorphous component on drawing causes a stiffening of the amorphous phase and a reduction of FFV. The consequence of this is a reduction of the zero-concentration diffusion coefficient and the appearance of sorption isotherms typical of glassy materials. As a consequence of the drastic decrease of the diffusion coefficient, the permeability of the fibers is much lower than that of the starting material. The good mechanical properties indicate a partial interconnection of the amorphous phases.

This work was supported by Ministero dell'Università e della Ricerca Scientifica e Tecnologica (PRIN 1998 titled "Stereoselective Polymerization: New Catalyst and New Polymeric Materials").

## REFERENCES

1. Ewen, J. A.; Jones, R. J.; Razavi, A.; Ferrara, J. D. *J Am Soc* 1988, 101, 6255.

2. Longo, P.; Proto, A.; Grassi, A.; Ammendola, P. *Macromolecules* 1992, 24, 462.
3. Grisi, F.; Longo, P.; Zambelli, A.; Ewen, J. A. *J Mol Cat A: Chemical* 1999, 140, 225.
4. Lovinger, A. J.; Lotz, B.; Davis, D. D. *Polymer* 1990, 31, 2253.
5. Chatani, Y.; Maruyama, H.; Noguchi, K.; Asanuma, T.; Shiomura, T. *J Polym Sci, Part C* 1990, 28, 393.
6. Auriemma, F.; Lewis, R. H.; Spiess, H. W.; De Rosa, C.; *Macromol Chem Phys* 1995, 196, 4011.
7. De Rosa, C.; F. Auriemma, Corradini, P.; *Makromol Chem* 1996, 29, 7452.
8. Lotz, B.; Lovinger, A. J.; Cais, R. E. *Macromolecules* 1988, 21, 2375.
9. Lovinger, A. J.; Davis, D. D.; Lotz, B. *Macromolecules* 1991, 24, 552.
10. De Rosa, C.; Corradini, P.; *Macromolecules* 1993, 26, 5711.
11. Nakaoki, T.; Ohira, Y.; Hayashi, H. *Macromolecules* 1998, 31(8), 2705.
12. Guadagno, L.; Fontanella, C.; Vittoria, V.; Longo, P. *J Polym Sci, Part C* 1999, 37, 173.
13. Guadagno, L.; D'Arienzo, L.; Vittoria, V. *Macromol Chem Phys*, 2000, 201, 246.
14. Uehara, H.; Yamazaki, Y.; Kanamoto, T. *Polymer* 1996, 37, 57.
15. Loos, J.; Huckert, A.; Petermann, J. *Colloid Polymer Sci* 1996, 274, 1006.
16. Loos, J.; Petermann, J.; Waldofner, A. *Colloid Polymer Sci* 1997, 275, 1088.
17. Loos, J.; Buhk, M.; Petermann, J.; Zoumis, K.; Kaminsky, W. *Polymer* 1996, 37, 387.
18. Guadagno, L.; D'Aniello, C.; Naddeo, C.; Vittoria, V., *Macromol. Rapid. Comm.*, 2001, 22, 1.
19. Thomann, R.; Kressler, J.; Setz, S.; Wang, C.; Mulhaupt, R. *Polymer* 1996, 37, 13.
20. Thomann, R.; Kressler, J.; Rudolf, B.; Mulhaupt, R. *Polymer* 1996, 37, 13.
21. Maier, R.; Thomann, R.; Kressler, J.; Mulhaupt, R.; Rudolf, B. *J Polymer Sci, Part B: Polym Phys* 1997, 35, 1135.
22. Bonnet, M.; Loos, J.; Petermann, J. *Colloid Polym Sci* 1998, 276, 524.
23. Phillips, R. A.; Jones, R. L. *Macromol Chem Phys* 1999, 200, 1912.
24. Williams, J. L.; Peterlin, A.; *J Polym Sci* 1971, A-2(9), 1483.
25. Araimo, L.; de Candia, F.; Vittoria, V.; Peterlin, A. *J Polym Sci Phys* 1978, 16, 2087.
26. de Candia, F.; Russo, R.; Vittoria, V.; Peterlin, A. *J Polym Sci Phys* 1982, 20, 269.
27. de Candia, F.; Perullo, A.; Vittoria, V.; Peterlin, A. *J Appl Polym Sci* 1983, 28, 1815.
28. de Candia, F.; Perullo, A.; Vittoria, V.; Peterlin, A. In *Interrelations between Processing Structure and Properties of Polymeric Materials*; Theocaris, J. C., Ed.; Elsevier: Amsterdam, 1984; p 713.
29. Choy, C. L.; Leung, W. P.; Ma, T. L. *J Polym Sci Phys* 1984, 22, 707.
30. Vittoria, V.; de Candia, F.; Capodanno, V. Peterlin, A. *J Polym Sci Phys* 1986, 24, 1009.
31. Vittoria, V. *Polymer* 1988, 29, 1119.
32. Natta, G.; Peraldo, G.; Corradini, P. *Rend Acc Naz Lincei* 1959, 26, 14.
33. D'Aniello, C.; Guadagno, L.; Naddeo, C.; Vittoria, V.; *Macromolecules* 2000, 33, 6023.
34. Crank, J.; Park, J. S. *Diffusion in Polymers*; Academic Press: London, 1968.
35. Peterlin, A. *J. Macromol Sci Phys* 1975, B11, 57.
36. Rogers, C. E. *Polymer Permeability*; Comyn, J., Ed.; Elsevier: London, 1985; Chapter 2.